

Thermodynamic study of the adsorption of Di-Azo dye on the activated carbon

Najm al-Din Abdullah saleh Amin¹, Bassam Abdel Razzaq Jamil Hussein², Homam T. S. AL-Sayd Toohe^{3*}

¹Directorate of Education in Aqrah, Iraq; ²Directorate of Education in Erbil, Iraq; ³Directorate of Education in Nineveh, Iraq

¹najmnak2@gmail.com; ²bassamgoran@gmail.com; ^{3*}homamtoohe@gmail.com

Abstract

The chemical structure of Al Qiayarah asphalt has been modified by catalytic treatment with mixtures of waste polymer (reclaimed tires rubber and polypropylene waste) mixture (1:1) (polymer: polymer) to make it more suitable for activated carbon preparation, prepared activated carbon properties were measured (adsorption of iodine number, methylene blue, density, ash content, and humidity) where we noticed a significant enhancement in its adsorption properties.

The Di-Azo dye (DAHNP) was prepared using 4-aminoantipyrine (4-AAP) and β -naphthol as major components, which reacted with α -aminophenol through diazotization and coupling reactions.

The optimized conditions of the adsorption system have been established, and the model of the Freundlich, Langmuir, and Tempkin adsorption isotherms was applied to determine the type of bonding between the surface of activated carbon and the adsorbed dye, as well as to exclude the adsorption system's natures.

The practical results show that the adsorption system is exothermically spontaneous and the binding force is physical.

The high correlation coefficient value (near 1) evidences the excellent applicability of the Langmuir isotherm, indicating the adsorption system is a mono-layer adsorption and the energy is homogeneously distributed on the surface of activated carbon.

Keywords: reclaimed tires rubber, polypropylene waste, thermal fusion carbonization, adsorption isotherms, Di-Azo dye, activated carbon.

Introduction

Industrial dyes are widely spread in industrial wastewater due to their complex composition, non-degradability, and water solubility. Some of their compounds, such as dyes, are important organic compounds that cause water pollution due to their widespread use in industries such as paper, plastic, rubber, cosmetics, food, and textile industries⁽¹⁾. Global consumption of textile fabrics currently stands at around 30 million tons per year, with expectations of further growth⁽²⁾. The presence of these dyes in wastewater poses a great danger; their removal from wastewater has become an urgent necessity⁽³⁾. The discharge of effluents from dyeing industries affects the

environment and pollutes water due to their high toxicity. Effluents contain many harmful chemicals that cause environmental problems⁽⁴⁾. Various techniques are used to remove dyes from wastewater, including chemical precipitation, ion exchange, osmosis, solvent extraction, membrane filtration, and adsorption⁽⁵⁾. Plastic and rubber waste pose a great danger to the ecological balance and the lives of living organisms due to their widespread use. It is characterized by its stability and non-decomposition after several years when found in soil or water. Thus, piles of plastic, car tires, and other causes of pollution spread throughout the world, to get rid of them, researchers focused on the possibility of benefiting from them, and thermal analysis methods are considered a modern method for recovering waste and using it to prepare and produce useful materials such as activated carbon, tire liner materials, asphalt additives, and others⁽⁶⁾. Adsorption is when a gaseous or liquid substance in the form of molecules, atoms, or ions of a substance called the adsorbent is collected on the surface of another porous solid substance called the adsorbent ⁽⁷⁾. Adsorption is one of the easiest and most efficient methods available at present; there is almost no industry without a special adsorption unit to treat and purify wastewater before it is introduced into the environment ⁽⁸⁾. Activated carbon is widely used as an adsorbent due to its high adsorption capacity in removing organic and inorganic pollutants from wastewater ⁽⁹⁾. The increasing interest in using low-cost materials available to produce activated carbon as an adsorbent has made adsorption a promising method. The efficiency of the adsorption process depends on the conditions under which adsorption takes place, such as contact time, temperature, acidity of the adsorption medium, pH, etc ⁽¹⁰⁾.

The type of adsorption system and the nature and manner of distribution of the adsorbent molecules on the solid surface of the adsorbent are usually determined by studying the adsorption at equilibrium and incorporating the experimental adsorption data into the isotherm equations that have been derived based on certain assumptions ⁽¹¹⁾.

Materials and methods

Preparation of diazo dyes

A: Preparation of monoazo dyes

The compound 4-aminoantipyrine was used as a base compound to prepare the dye as follows:

First: Preparation of the diazonium salt

Dissolve (3) grams of 4-aminoantipyrine in (10 ml) concentrated hydrochloric acid and (2) ml (distilled water while maintaining the temperature of the solution in an ice bath (0-5°C), add (1) grams of sodium nitrite in (5) ml) distilled water while maintaining the temperature (0-5°C)

Second: Preparation of the α -aminonaphthol solution

Prepare (9 ml) sodium hydroxide concentration 10% in an ice bath and add (1.6 grams) of α -aminonaphthol while maintaining the reaction temperature (0-5°C). Add the diazonium salt solution to the solution of the second step with stirring until the crystals of the required substance are formed. Leave the mixture for an hour in an ice bath, filter and wash with distilled water, and dry.

B. Preparation of the diazolidinyl dye

Step one: Preparation of Diazonium salt

A- Dissolve (0.322 g) of 4-aminoantipyrine azoP-aminophenol in (10 ml) hydrochloric acid while maintaining the temperature (0-5°C).

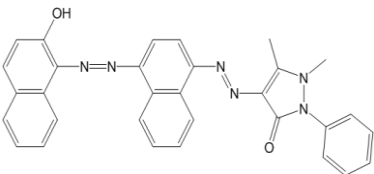
B- Add (1 g) of sodium nitrite to (10 ml) of distilled water at a temperature of (0-5°C). This solution is added gradually and slowly to the first solution in an ice bath.

Step two: Prepare a solution of β -naphthol

(9 ml) of 10% sodium hydroxide solution in an ice bath and add (0.4 g) of β -naphthol.

The solution of the first step is added to the second step gradually, and the mixture is left in an ice bath, filtered, washed with distilled water, and dried.

Table (1): Represents the name, composition and some physical properties of the dye (DAHNP).

Dye name	Structure of dye	Colour	M.P °C	λ_{Max} (nm)	M.Wt g/mol	ϵ_{max} L/mol.cm
4-((1E)-4-((2-hydroxynaphthalen-1-yl)diazenyl)naphthalen-1-yl)diazenyl)-1,5-dimethyl-2-phenyl-1H-pyrazol-3(2H)-one		Black	100-102	396	512.6	6969.4

Preparation of activated carbon:

The asphalt was treated with a mixture of recycled tire rubber and polypropylene, where the polymers were mixed in a ratio of 1:1 (polymer: polymer), then added to the asphalt in proportions ranging between (0.5-3% by weight) and with an increase of (0.5% by weight) and in the presence of (0.06%) anhydrous aluminum chloride catalyst at a temperature of (180 °C) with continuous shaking for half an hour, after which the samples were placed in a microwave oven for 15 minutes at a power of (360) watts, the asphaltene was separated for all the prepared samples, where 1 gram of modified asphalt was placed and dissolved in 40 ml of petroleum ether solvent (80-60 °C) at a ratio of (40:1) (weight: volume) shaking for 3 hours at (25 °C), the asphaltene was separated by filtration and the percentage of the samples was calculated (12). The best sample in terms of asphaltene content was taken, and distillation processes were carried out under normal atmospheric pressure to remove as many light components as possible. After distillation under atmospheric pressure, the resulting residue was distilled under low pressure (20 mm Hg), and the remaining material was used in preparing activated carbon (13). The remaining material was taken from the distillation under vacuum pressure and placed in a ceramic flask with potassium hydroxide in a ratio of (2:1) [vacuum distillation residues: potassium hydroxide], then heated in a tightly sealed electric furnace to a temperature of (350°C) for three hours, then the flask was transferred to the complementary carbonization stage where it was heated to a temperature of (700°C) for two hours. Based on our previous study, the prepared activated carbon was purified and the alkaline pollutant and mineral components were removed (14). The prepared carbon was reactivated by heating in the microwave using a power of 720 watts and a time of half an hour.

The effectiveness of activated carbon models was determined by measuring the internal surface area of activated carbon by adsorption of iodine from its aqueous solution (15), measuring the external surface area of activated carbon by measuring the adsorption capacity of methylene blue dye from its aqueous solution (16), measuring density (17), ash content (18), and moisture percentage (19).

Results and discussion

Thermodynamic study of dye adsorption on prepared activated carbon:

The aim of the study is to determine the optimum conditions for the adsorption system, including determining the amount of adsorbent, contact time, initial concentration and the effect of temperature on adsorption.

Analytical method

Using the spectroscopic method in the visible region, including making a calibration curve for the dye at (λ_{\max}) by preparing solutions with concentrations of [1×10^{-4} - 1×10^{-5}] molar. And plotting the absorbance versus concentration according to the Beer-Lambert law (20).

$$A = \varepsilon bC \dots \dots \dots (1)$$

A is the dye absorbance and molar absorption coefficient ($\text{Liter.mol}^{-1}.\text{cm}^{-1}$), b is the visible light path length (1cm), and C is the molar concentration (mol/Liter). A solvent of a mixture of (50% water/ethanol) was used, Figure (1) Calibration curve for the dye (DAHNP)

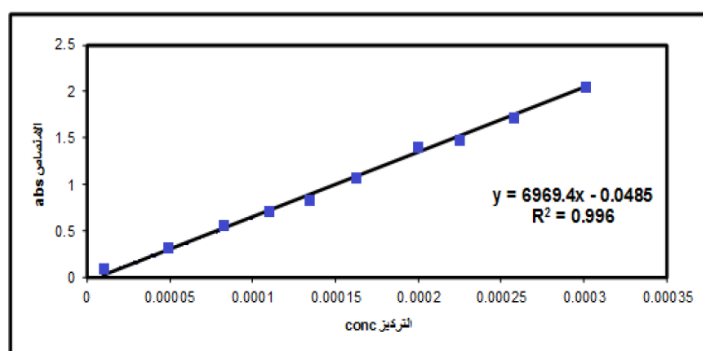


Fig. 1: Calibration curves of the studied dye(DAHNP).

Effect of adsorbent dose:

The effect of the amount of adsorbent was studied in determining the optimum amount required to reach the equilibrium state of the adsorption system without completely removing the dye while maintaining the color. Table (2) represents the effect of the amount of adsorbent, where we notice an increase in the percentage of adsorption and adsorption capacity with increasing the amount of adsorbent in a fixed volume. This is due to the increase in the effective active site on the carbon surface. (0.5) grams represents the appropriate and approved amount to complete the study (21). The results are in Table 3.

Table (2): Effect of the amount of activated carbon on the adsorption of dye (DAHNP) at a temperature of 20°C, an initial concentration of (4×10^{-4} M) and a shaking time of 30min.

Dose (gm/L)	C _i (mg/L)	C _e (mg/L)	C _{ads} (mg/L)	q _e (mg/g)	%Ads
0.25	153.78	33.063	120.717	241.435	78.50
0.5		13.671	140.109	280.218	91.11
0.75		7.689	146.091	292.182	95.00
1		5.844	147.936	295.873	96.20
2		4.613	149.167	298.333	97.00

Effect of contact time:

The effect of contact time was studied at different temperatures and initial concentration (4×10^{-4} M), activated carbon weight 0.5 g/L, and times (70-10) minutes. We notice that the reaction reaches equilibrium at 70 minutes, where the rate of binding of dye molecules to the surface of activated carbon is equal to the rate of emission of other molecules from the surface into the solution. This is called equilibrium. The results are in Table 3. Table (3): Effect of contact time on adsorption capacity at (20-60°C) and initial concentration (4×10^{-4} M), activated carbon weight 0.5 g/L, and shaking speed 100 rpm.

T (°C)	Time (min)	Ct (mg/L)	qt (mg/g)	%Ads
20	5	93.621	187.243	60.88
	10	119.948	239.897	78.00
	15	124.439	248.878	80.92
	20	130.713	261.426	85.00
	25	136.680	273.359	88.88
	30	140.109	280.218	91.11
	35	140.478	280.956	91.35
	40	140.478	280.956	91.35
30	5	92.652	185.305	60.250
	10	119.303	238.605	77.58
	15	124.162	248.324	80.74
	20	129.129	258.258	83.97
	25	136.095	272.191	88.50
	30	139.294	278.588	90.58
	35	140.094	280.187	91.10
	40	140.094	280.187	91.10
40	5	92.483	184.967	60.14
	10	118.841	237.682	77.28
	15	123.362	246.725	80.22
	20	127.207	254.414	82.72
	25	135.019	270.038	87.80
	30	136.587	273.175	88.82
	35	139.940	279.880	91.00
	40	139.940	279.880	91.00
50	5	92.286	184.573	60.012
	10	117.413	234.825	76.351
	15	121.486	242.972	79.00
	20	126.300	252.599	82.13
	25	133.358	266.716	86.72
	30	135.788	271.575	88.30
	35	138.571	277.142	90.11
	40	138.556	277.112	90.10
60	5	91.896	183.792	59.758
	10	117.107	234.213	76.152
	15	121.317	242.634	78.89
	20	123.793	247.586	80.50
	25	132.405	264.809	86.10
	30	135.326	270.653	88.00
	35	138.402	276.804	90.00
	40	138.402	276.804	90.00

Effect of initial concentration.

The range of concentrations studied was from 2×10^{-4} to 7×10^{-4} molar after fixing all other variables. The results are listed in Table 5. We notice that with increasing concentration, the adsorption efficiency decreases. This is due to the fact that with increasing concentration, the adsorbed molecules that compete to bind to the active sites on the carbon surface increase. Thus, the concentration of the remaining dye in the solution (22) is 3×10^{-4} , which is considered the optimal concentration that is adopted in this study while keeping the color within the required limits.

Table (4): Effect of initial concentration on adsorption percentage at 20°C, activated carbon weight 0.5 g/L, and shaking time 40 min.

C_i (mol/L)	C_i (mg/L)	C_e (mg/L)	C_{ads} (mg/L)	q_e (mg/g)	%Ads
2×10^{-4}	102.52	5.126	97.394	194.788	95.00
3×10^{-4}	153.78	16.916	136.864	273.728	89.00
4×10^{-4}	205.04	37.112	167.928	335.856	81.90
5×10^{-4}	256.3	55.105	201.196	402.391	78.50
6×10^{-4}	307.56	76.890	230.670	461.340	75.00
7×10^{-4}	358.82	111.234	247.586	495.172	69.00

Effect of pH

The effect of acidity function was studied in three acidic media (pHNatural, 7,9) at constant temperature and concentration, the results are listed in Table (5). Table (5): Effect of acidity function on adsorption capacity at 20°C and initial concentration (3×10^{-4} M) and shaking time 40 minutes and activated carbon weight 0.5 g/L and shaking speed 100 rpm.

pH	C_i (mg/L)	C_e (mg/L)	C_{ads} (mg/L)	q_e (mg/g)	%Ads
5.2*	153.78	12.302	141.478	282.955	92.00
7		31.525	122.255	244.510	79.50
9		50.440	103.340	206.680	67.20

pH Natural*

From the table, we notice that the adsorption efficiency is high at the natural acidity function (5.2) much higher than the neutral and basic acidity functions, where in the acidic medium the protons (positive charge) are the dominant charge in the solution, as the phenolic groups in the dye are transformed into the positively charged phenoxynium ion. We conclude that the surface of the prepared carbon is negatively charged, based on the concept that different charges attract each other, and thus the interference increases and the adsorption efficiency increases ⁽²³⁾.

Effect of Temperature on Adsorption:

Studying the effect of temperature is important for the purpose of studying the specifications of the adsorption system, calculating the thermodynamic functions, and applying adsorption isotherms. The study was conducted over a range of temperatures (20-60°C) with other variables fixed. The results are listed in Table 6.

Table (6): Effect of temperature on the percentage of adsorption at pHNatural, shaking time 40 minutes, activated carbon weight 0.5 g/L, and shaking speed 100 rpm.

C_i (mol/L)	C_i (mg/L)	Temp (°C)	C_e (mg/L)	C_{ads} (mg/L)	q_e (mg/g)	% Ads
3×10^{-4}	153.78	20	13.302	140.478	280.956	91.35
		30	13.686	140.094	280.187	91.10
		40	13.840	139.940	279.880	91.00
		50	15.224	138.556	277.112	90.10
		60	15.378	138.402	276.804	90.00

We observe a decrease in the efficiency and capacity of adsorption with increasing temperature, due to the breaking of the bonding forces between the dye and the carbon surface, and the return of the dye molecules to the solution. This indicates that the adsorption system is exothermic and the nature of adsorption is physical (24).

Calculating the thermodynamic functions of adsorption:

The thermodynamic functions of the adsorption system at equilibrium were found through the equilibrium constant (K), which is calculated from the ratio between the concentration of the adsorbed dye over the remaining in the solution at (20-60°C) and the concentration of ($3 \times 10^{-4} \text{M}$) with the other variables fixed. The results are listed in Table 7, Figure 2. The relationship between $\ln K$ and $1/T$ is used to calculate the value of the adsorption enthalpy of the dye (DAHNP).

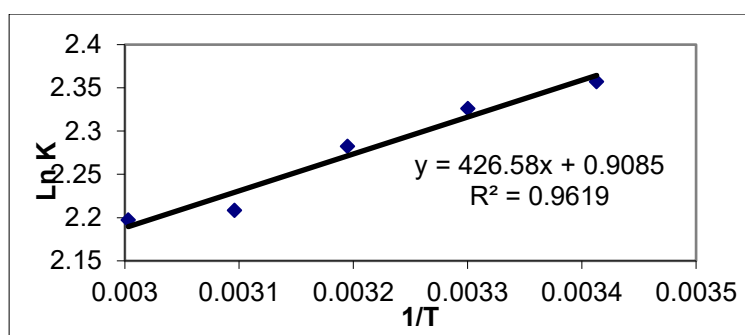


Figure 4: The relationship between $\ln K$ versus ($1/T$) to calculate the values of the adsorption enthalpy of dye (DAHNP).

Table (7): Values of thermodynamic functions at equilibrium for the adsorption of the dye (DAHNP) on the activated carbon prepared at a concentration of (3×10^{-4}) molar and at (20-60°C).

C_i (mol/L)	Temp °K	K	$H \Delta$ (KJ.mol ⁻¹)	$S \Delta$ (J.mol ⁻¹ .K ⁻¹)	$G^\circ \Delta$ (KJ.mol ⁻¹)	ΔS° (J.mol ⁻¹ .K ⁻¹)
3×10^{-4}	293	10.561	-6.640	-22.661	-5.742	-3.064
	303	10.236		-21.914	-5.859	-2.576
	313	9.800		-21.213	-5.939	-2.238
	323	9.101		-20.557	-5.930	-2.196
	333	9.000		-19.939	-6.083	-1.672

From Table (7), the negative sign of $H \Delta$ indicates that the reaction is exothermic, and the numerical value indicates that the forces responsible for adsorption are of a physical nature. The sign of $S \Delta$ is also negative, which indicates the regularity of the adsorption system. With increasing temperature, we observe a slight increase in its values, which is attributed to the disengagement between the dye and the adsorbent surface and the return of the dye molecules to the solution (26,25). The negative sign of the free energy of $G^\circ \Delta$ indicates the spontaneity of the adsorption system within the range of temperatures studied (27).

Adsorption isotherms:

Three types of adsorption isotherm models were applied in this study (Freundlich, Langmuir, and Temkin), each of which is based on certain assumptions that differ according to the type of isotherm and is applied depending on the experimental data of the adsorption system.

Freundlich isotherm:

Freundlich isotherm was applied according to equation (2) by plotting the relationship between $\log q_e$ versus $\log C_e$ (28), Freundlich constants values (K_f , n) were calculated from the slope and line segment. The results are shown in Figure (3) and Table (8).

$$\log q_e = \log K_f + \frac{1}{n} \log C_e \text{ ----- (2)}$$

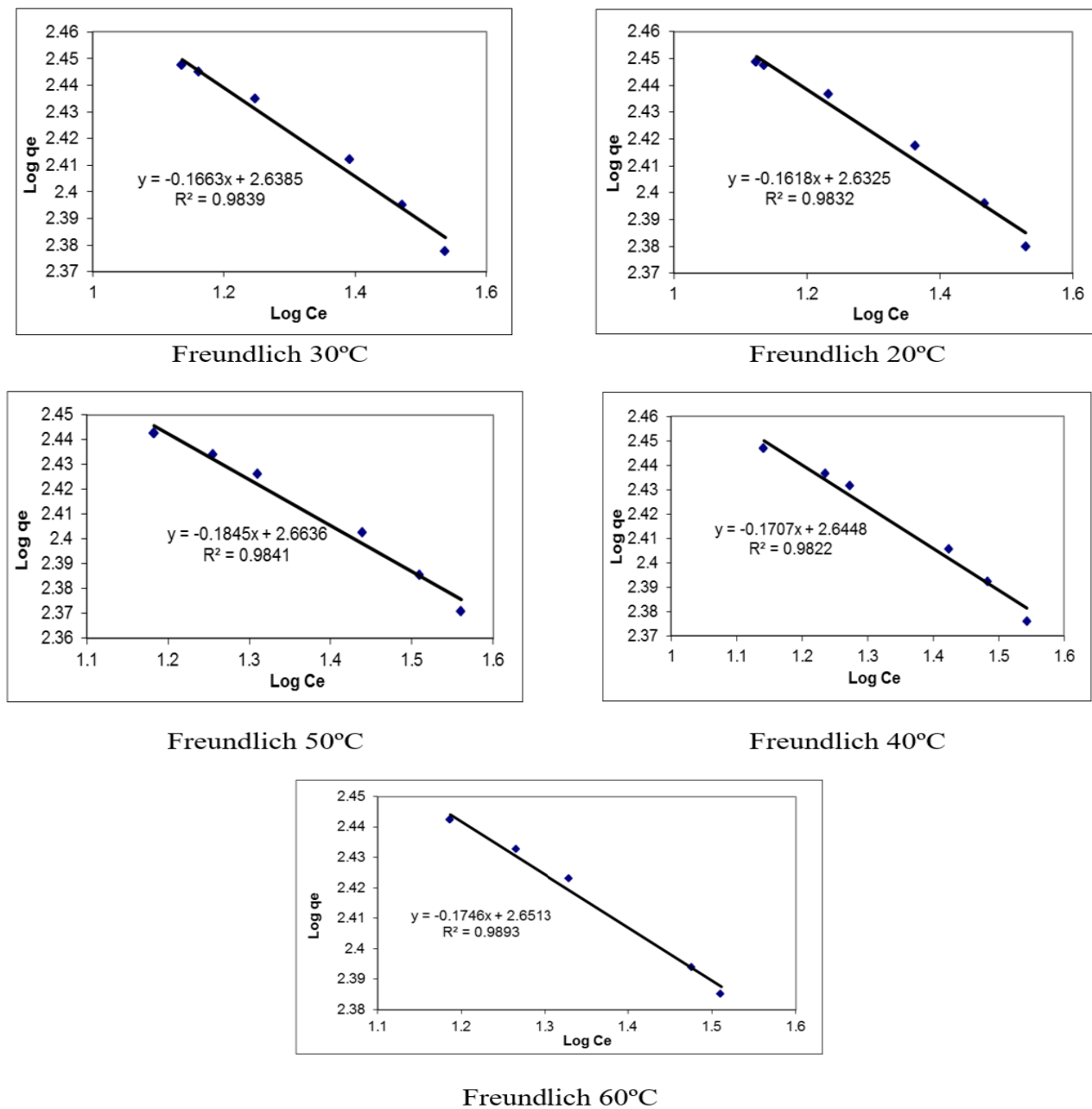


Figure (3): Freundlich isotherm for dye adsorption (DAHNP)

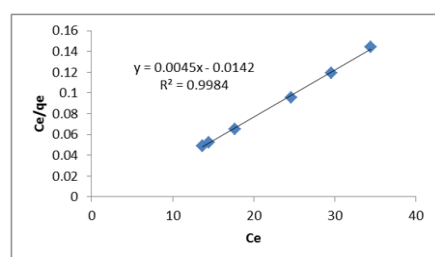
Table (8): Values of Freundlich constants (n, K_f) and correlation coefficients.

Temp.(°C)	n	K _f	R ²
20	-6.180	429.042	0.9832
30	-6.013	435.011	0.9839
40	-5.858	441.367	0.9822
50	-5.420	460.893	0.9841
60	-5.727	427.858	0.9893

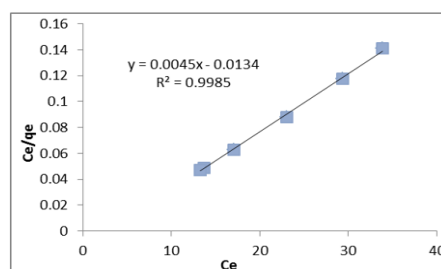
Langmuir isotherm: The Langmuir isotherm was applied by plotting the relationship between C_e/q_e versus C_e according to equation (3) under the same conditions that were applied using the Freundlich isotherm.

The results are listed in Table No. (9) and the graphs obtained from this equation are shown in Figure 4.

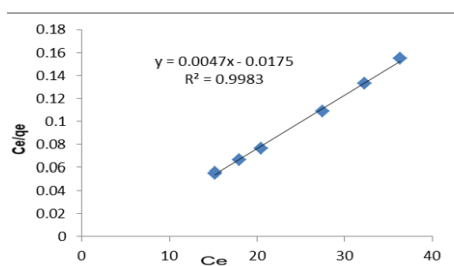
$$\frac{C_e}{q_e} = \frac{1}{b Q_{\max}} + \frac{C_e}{Q_{\max}} \quad \text{.....(3)}$$



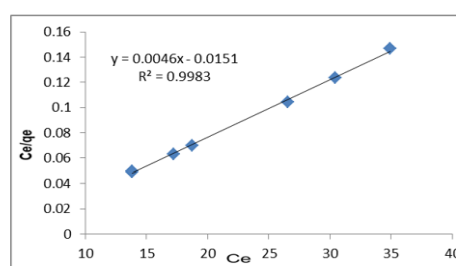
Langmuir 30°C



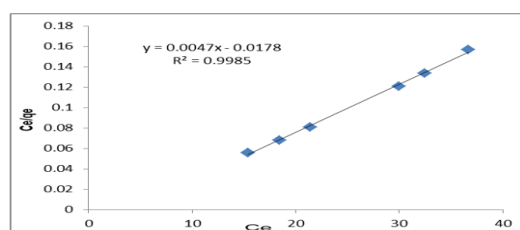
Langmuir 20°C



Langmuir 50°C



Langmuir 40°C



Langmuir 60°C

Figure (4): Langmuir isotherm for dye adsorption (DAHNP)

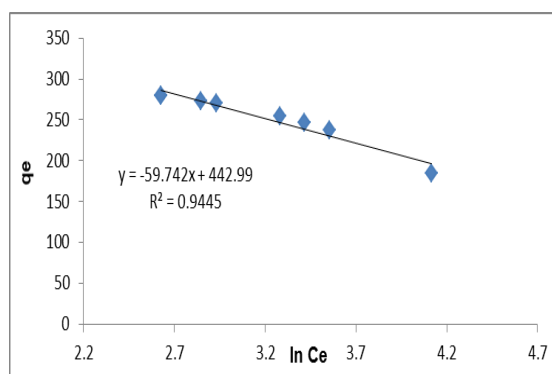
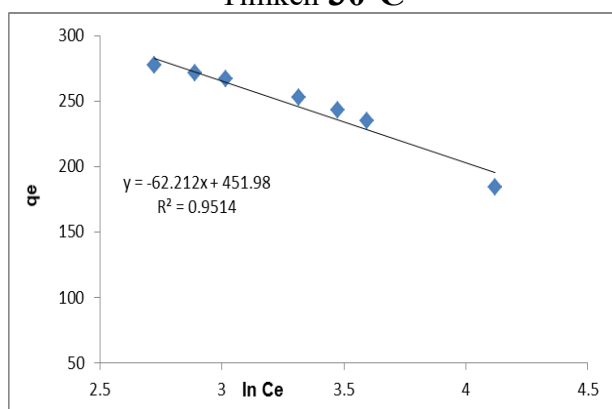
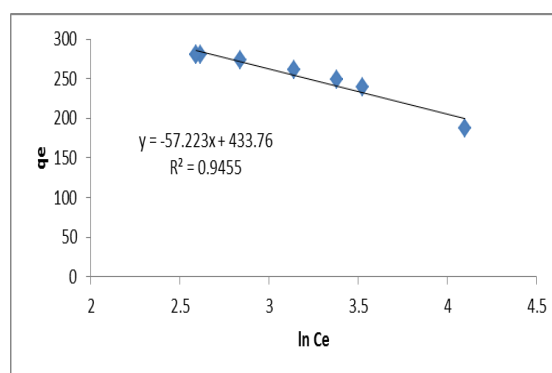
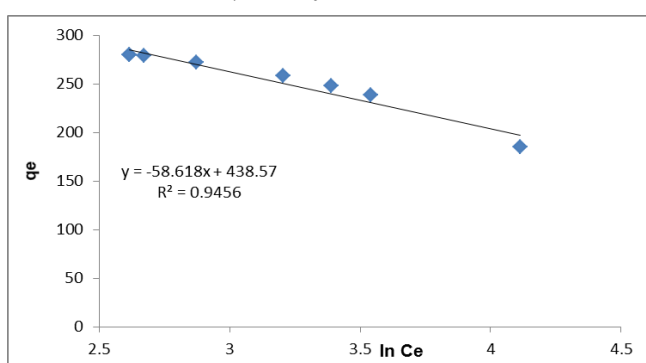
Table (9): Values of Langmuir constants (Q_{\max}) and (b) and correlation coefficients.

Temp.(C°)	b(L/mg)	Q_{\max} (mg/g)	R^2
20	-0.3358	-2.9778	0.9985
30	-0.3169	-3.1556	0.9984
40	-0.3046	-3.2826	0.9983
50	-0.1323	-7.5593	0.9983
60	-0.1285	-7.7797	0.9985

Isotherm Timken:

The Temkin isotherm was applied using equation (4) and by drawing the relationship between q_e versus $\ln C_e$, and from the slope and the intercept of the straight lines the values of the Temkin constants were calculated. The results are listed in Table (10) and the graphs in Figure (5).

$$q_e = B_T \ln K_T + B_l \ln C_e \text{----- (4)}$$



Timken 50°C

Timken 40°C

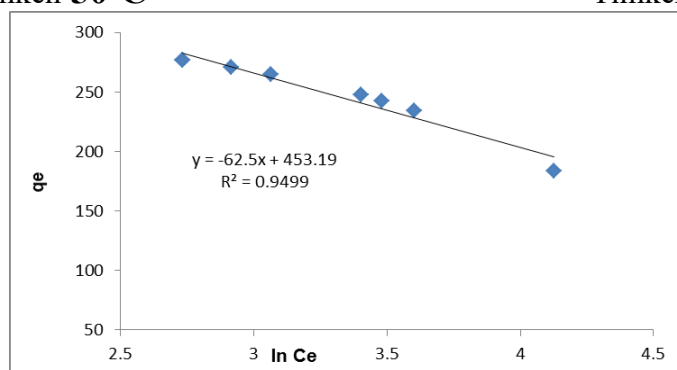


Figure (5): Timken isotherm for dye adsorption (DAHNP)

Table (10): Values of the Temkin constants (BT, KT) and correlation coefficients

Temp.(C°)	B _T	K _T (Liter/mg)	R ²
20	-57.2230	0.001	0.9455
30	-58.6180	0.001	0.9456
40	-59.7420	0.001	0.9445
50	-62.2120	0.001	0.9514
60	-62.5000	0.001	0.9499

By applying three types of adsorption isotherm models, we notice that the Langmuir isotherm is largely applicable through the high correlation coefficient values. This means that the adsorption system is a monolayer and the energies of the active sites on the surface of the adsorbent are equivalent in energy (30,29).

References

1. Pattanshetti, A., Koli, A., Dhabbe, R., Yu, X. Y., Motkuri, R. K., Chavan, V. D., ... & Sabale, S. (2024). Polymer Waste Valorization into Advanced Carbon Nanomaterials for Potential Energy and Environment Applications. *Macromolecular Rapid Communications*, 45(7), 2300647.
2. Sathiyavimal, S., Durán-Lara, E. F., Vasantharaj, S., Saravanan, M., Sabour, A., Alshiekheid, M., ... & Pugazhendhi, A. (2022). Green synthesis of copper oxide nanoparticles using Abutilon indicum leaves extract and their evaluation of antibacterial, anticancer in human A549 lung and MDA-MB-231 breast cancer cells. *Food and Chemical Toxicology*, 168, 113330.
3. James, N., Mwangi, I. W., Wanjau, R. N., & Murungi, J. I. (2021). Adsorption studies of p-Nitrophenol from Model aqueous solutions using Raw and Quaternised thorn melon (*Cucumis metuliferus*) peels.
4. Kim, S. H., Kim, D. S., Moradi, H., Chang, Y. Y., & Yang, J. K. (2023). Highly porous biobased graphene-like carbon adsorbent for dye removal: Preparation, adsorption mechanisms and optimization. *Journal of Environmental Chemical Engineering*, 11(2), 109278.
5. Shen, Y., Li, B., & Zhang, Z. (2023). Super-efficient removal and adsorption mechanism of anionic dyes from water by magnetic amino acid-functionalized diatomite/yttrium alginate hybrid beads as an eco-friendly composite. *Chemosphere*, 336, 139233.
6. Danila, V., & Januševičius, T. (2023). Adsorption of aqueous Pb (II) using non-devulcanized and devulcanized tyre rubber powder: A comparative study. *Environmental Science and Pollution Research*, 1-17.
7. Ahmad, A. A., Al-Raggad, M., & Shareef, N. (2021). Production of activated carbon derived from agricultural by-products via microwave-induced chemical activation: a review. *Carbon Letters*, 31(5), 957-971.
8. Agarwala, R., & Mulky, L. (2023). Adsorption of dyes from wastewater: A comprehensive review. *ChemBioEng Reviews*, 10(3), 326-335.
9. Thi Tuyet Nhi, N., Thi Mai Tho, N., & Thi Hong Anh, N. (2024). An efficient adsorbent for the removal of dyes prepared by an in situ growth of ZIF-8 onto activated carbon. *Green Chemistry Letters and Reviews*, 17(1), 2377555.

10. Kumar, N., Pandey, A., & Sharma, Y. C. (2023). A review on sustainable mesoporous activated carbon as adsorbent for efficient removal of hazardous dyes from industrial wastewater. *Journal of Water Process Engineering*, 54, 104054.
11. Ramesh, P., Padmanabhan, V., Saravanan, P., & Thillainayagam, B. P. (2023). Batch studies of turquoise blue dye (TB) adsorption onto activated carbon prepared from low-cost adsorbents: an ANN approach. *Biomass Conversion and Biorefinery*, 13(4), 3267-3280.
12. Qajar, J., Razavifar, M., & Riazi, M. (2024). A mechanistic study of the synergistic and counter effects of ultrasonic and solvent treatment on the rheology and asphaltene structure of heavy crude oil. *Chemical Engineering and Processing-Process Intensification*, 195, 109619.
13. Bustillo Revuelta, M., & Bustillo Revuelta, M. (2021). Bituminous Materials. *Construction Materials: Geology, Production and Applications*, 401-434.
14. Toohi, H. T. A. S., Rabeea, M. A., Abdullah, J. A., & Muslim, R. F. (2021). Synthesis and characterization activated carbon using a mix (asphalt-polypropylene waste) for novel azo dye (HNDA) adsorption. *Carbon Letters*, 31(5), 837-849.
15. Corda, N. C., & Kini, M. S. (2018). A review on adsorption of cationic dyes using activated carbon. In *MATEC web of conferences* (Vol. 144, p. 02022). EDP Sciences.
16. Haskis, P., Ioannidis, I., Mpeza, P., Giannopoulos, G., Barouchas, P., Selvasembian, R., ... & Anastopoulos, I. (2024). Agricultural Biomass/Waste-Derived Adsorbents for the Abatement of Dye Pollutants in (Waste) Water. In *Planet Earth: Scientific Proposals to Solve Urgent Issues* (pp. 161-183). Cham: Springer International Publishing.
17. Musa, S. A., Abdulhameed, A. S., Baharin, S. N. A., ALOthman, Z. A., Selvasembian, R., & Jawad, A. H. (2024). Pyrolyzed coal base high surface area and mesoporous activated carbon for methyl violet 2B dye removal: Optimization of preparation conditions and adsorption key parameters. *Chemical Engineering Research and Design*, 205, 67-78.
18. Matias, P. M., Sousa, J. F., Bernardino, E. F., Vareda, J. P., Durães, L., Abreu, P. E., ... & Valente, A. J. (2023). Reduced chitosan as a strategy for removing copper ions from water. *Molecules*, 28(10), 4110.
19. Bian, P., & Shao, Q. (2024). Efficient adsorption of hexavalent chromium in water by torrefaction biochar from lignin-rich kiwifruit branches: The combination of experiment, 2D-COS and DFT calculation. *International Journal of Biological Macromolecules*, 273, 133116.
20. Shakya, A. K., & Singh, S. (2024). Performance analysis of a developed optical sensing setup based on the Beer-Lambert law. *Plasmonics*, 19(1), 447-455.
21. Umeh, A. C., Hassan, M., Egbuatu, M., Zeng, Z., Al Amin, M., Samarasinghe, C., & Naidu, R. (2023). Multicomponent PFAS sorption and desorption in common commercial adsorbents: Kinetics, isotherm, adsorbent dose, pH, and index ion and ionic strength effects. *Science of the Total Environment*, 904, 166568.
22. Mozhiarasi, V., & Natarajan, T. S. (2024). Bael fruit shell-derived activated carbon adsorbent: effect of surface charge of activated carbon and type of pollutants for improved adsorption capacity. *Biomass Conversion and Biorefinery*, 14(7), 8761-8774.
23. Al-Hazmi, G. A., El-Zahhar, A. A., El-Desouky, M. G., & El-Bindary, A. (2024). Superior adsorption and removal of doxorubicin from aqueous solution using activated carbon via thermally treated green adsorbent: isothermal, kinetic, and thermodynamic studies. *Environmental Technology*, 45(10), 1969-1988.

24. Gohr, M. S., Abd-Elhamid, A. I., El-Shanshory, A. A., & Soliman, H. M. (2022). Adsorption of cationic dyes onto chemically modified activated carbon: Kinetics and thermodynamic study. *Journal of Molecular Liquids*, 346, 118227.
25. Sha, A. A., & Baiju, V. (2021). Thermodynamic analysis and performance evaluation of activated carbon-ethanol two-bed solar adsorption cooling system. *International Journal of Refrigeration*, 123, 81-90.
26. Feizbakhshan, M., Amdebrhan, B., Hashisho, Z., Phillips, J. H., Crompton, D., Anderson, J. E., & Nichols, M. (2021). Effects of oxygen impurity and desorption temperature on heel build-up in activated carbon. *Chemical Engineering Journal*, 409, 128232.
27. Abdelaziz, G. B., El-Said, E. M., Bedair, A. G., Sharshir, S. W., Kabeel, A. E., & Elsaid, A. M. (2021). Experimental study of activated carbon as a porous absorber in solar desalination with environmental, exergy, and economic analysis. *Process Safety and Environmental Protection*, 147, 1052-1065.
28. Cuadrado-Collados, C., Farrando-Pérez, J., Martínez-Escandell, M., Missyul, A., & Silvestre-Albero, J. (2020). Effect of additives in the nucleation and growth of methane hydrates confined in a high-surface area activated carbon material. *Chemical Engineering Journal*, 388, 124224.
29. Al-Hyali, E. A., AL-Memary, K. A., & AL-Sayd Toohi, H. T. A. (2020). Preparation of Activated Carbon From ((Asphalt: Polymer)) Mixtures and Improving its Adsorption Properties by Thermal Fusion Carbonization and Microwave Technique. *Journal of Education and Science*, 29(1), 233-241.
30. Al-Hyali, E. A., AL-Memary, K. A., & AL-Sayd Toohi, H. T. A. (2020). Preparation of Activated Carbon From ((Asphalt: Polymer)) Mixtures and Improving its Adsorption Properties by Thermal Fusion Carbonization and Microwave Technique. *Journal of Education and Science*, 29(1), 233-241.